JGR: Planets

Supporting Information for

Amorphization of S, Cl-salts Induced by Martian Dust Activities

Alian Wang[1], Yuanchao Yan[1], Darby M. Dyar[2], Jen L. Houghton[1], William M. Farrell[3], Bradley L. Jolliff[1], Scott M. McLennan[4], Erbin Shi[1,5], Hongkun Qu[1,5]

[1]Dept. Earth & Planetary Sciences and McDonnell Center for the Space Sciences, Washington University in St. Louis (alianw@levee.wustl.edu),

[2]Planetary Science Institute, 1700 E. Fort Lowell, Suite 106, Tucson, AZ 85719.

[3]Solar System Exploration Division, Goddard Space Flight Center (GSFC), NASA, USA.

[4]Dept. Geoscience, Stony Brook University, Stony Brook, NY 11794

[5]Dept. Physics and Space Sciences, Shandong University at Weihai, China.

Contents of this file

Introduction

This supporting information document contains two tables and eight figures that provide additional information for the observations presented in this manuscript.

Table S1 lists the derived electron flux in the ESD experiments based on the current measurement (~ 22 mA, same value to that of Wu et al., 2018), which is 1.42×10^{20} $s^{-1}m^{-2}$. When compared with the calculated electron fluxes based on modeled value for ESD-*Townsend dark discharge (TDD) and ESD-normal glow discharge (NGD)(Delory et al., 2006),* 9×10^{16} $s^{-1}m^{-2}$ *(TDD)* and 1.5×10^{24} $s^{-1}m^{-2}$ *(NGD)*, we can conclude that the electron flux density realized in our experiments has a strength mid-way between ESD-TDD and ESD-NGD.

Table S2 lists the Weibull probability density function calculated used the Weibull parameters obtained from the curve fit of REMS data from sol 9 to sol 1474 (1465 sols =2.19 Mars year): Cc=6.87 m/s, k=1.73, into the Weibull probability density function: f(v)=(k/c)(v/c)^(k-1)exp(-(v/c)^k). (Viudex-Mpreiras et al., 2019)

Figure S1 supports section 4.2.1 ESD products from FeSO4.xH2O (x=1, 4, 7), especially the Mossbauer analysis results.

Figure S2-S6 support section 4.1.3.2 ESD products from Na-jarosite, akaganeite, and pyrite that show no obvious phase changes after 7h, 14h, 64h ESD processes on those minerals.

Figure S7 support the discussion in section 6. Implications for martian dust activities, especially about the major differences between Townsend dark discharge (TDD), or normal glow discharge (NGD) is in electron flux density (Gallo 1975).

Figure S8 (from Figure 4 of Wu et al., 2018) supports the statement in abstract and section 2 on the generation of "free Radicals" by ESD process in CO_2, CO_2+H_2O, and MSGM, shown as their emission lines in plasma spectra.

Table S1. Calculated electron flux of our ESD experiments which is same as Wu et al (2018) compared with modeled ESD-TDD and ESD-NGD (Delory et al., 2006).

ESD-NGD of Wu et al., 2018:					
current in mA	**current in C/s**	**number of electron per second (1/s)**	**electrode diameter (m)**	**electrode area (m^2)**	**electron flux (number of electron/(s*m ^2))**
22	0.022	1.37E+17	0.035	0.000962	**1.43E+20**
Delory et al., 2006, Figure 4 & 5					
			electron drift velocity (m/s) by Delory model [3]	**electron density (Ne/m^3) by Delory model**	**electron flux (number of electron/(s*m ^2)) by Delory model**
BEFT of ESD_TDD = 25 kV/m (Farrell et al., 2015)			3.00E+05	3.00E+11	**9.00E+16**
BEFT of ESD_NGD = 34 kV/m (Yan et al., 2017)			3.00E+05	5.00E+18	**1.50E+24**

[1]. 1 ampere (A) =1 Coulomb/s, 1 Coulomb =6.238729x10^{18} electron charge, 1 eV =1.6x10^{-19} Joule
[2]. Electrode: diameter=0.035mm, area=0.000962 m^2
[3]. Assuming the electron drift velocities for ESD-TDD and ESD-NGD are very similar

Table S2. MSL_REMS Weibull probability density function (Viudex-Mpreiras et al., 2019)

Weibull probability density function: f(v)=(k/c)(v/c)^(k-1)exp(-(v/c)^k)

The obtained Weibull Parameters based on curve fit of REMS data from sol 9 to sol 1474 (1465 sols =2.19 Mars year): Cc=6.87 m/s, k=1.73

v (m/s)	k/c	v/c	(v/c)^k-1	(v/c)^k	exp(-(v/c)^k)	**f(V)**	**area**	**< 3.5 m/s**	**< 5 m/s**	**< 7 m/s**	**< 10 m/s**	**< 15 m/s**	**< 20 m/s**
0	0.2518	0.0000	0.0000	0.0000	1.0000	0.0000							
0.5	0.2518	0.0728	0.1477	0.0107	0.9893	0.0368	0.0184						
1	0.2518	0.1456	0.2449	0.0357	0.9650	0.0595	0.0298						
1.5	0.2518	0.2183	0.3293	0.0719	0.9306	0.0772	0.0386						
2	0.2518	0.2911	0.4062	0.1183	0.8885	0.0909	0.0454						
2.5	0.2518	0.3639	0.4781	0.1740	0.8403	0.1012	0.0506						
3	0.2518	0.4367	0.5462	0.2385	0.7878	0.1084	0.0542						
3.5	0.2518	0.5095	0.6112	0.3114	0.7324	0.1127	0.0564	**0.2933**					
4	0.2518	0.5822	0.6738	0.3923	0.6755	0.1146	0.0573						
4.5	0.2518	0.6550	0.7343	0.4810	0.6182	0.1143	0.0572						
5	0.2518	0.7278	0.7930	0.5771	0.5615	0.1121	0.0561		**0.4638**				
5.5	0.2518	0.8006	0.8501	0.6806	0.5063	0.1084	0.0542						
6	0.2518	0.8734	0.9059	0.7912	0.4533	0.1034	0.0517						
6.5	0.2518	0.9461	0.9604	0.9087	0.4031	0.0975	0.0487						
7	0.2518	1.0189	1.0138	1.0330	0.3560	0.0909	0.0454			**0.6639**			
7.5	0.2518	1.0917	1.0661	1.1639	0.3123	0.0838	0.0419						
8	0.2518	1.1645	1.1176	1.3014	0.2722	0.0766	0.0383						
8.5	0.2518	1.2373	1.1681	1.4453	0.2357	0.0693	0.0347						
9	0.2518	1.3100	1.2179	1.5955	0.2028	0.0622	0.0311						
9.5	0.2518	1.3828	1.2670	1.7520	0.1734	0.0553	0.0277						
10	0.2518	1.4556	1.3153	1.9145	0.1474	0.0488	0.0244				**0.8620**		
10.5	0.2518	1.5284	1.3630	2.0832	0.1245	0.0427	0.0214						
11	0.2518	1.6012	1.4101	2.2577	0.1046	0.0371	0.0186						
11.5	0.2518	1.6739	1.4566	2.4382	0.0873	0.0320	0.0160						
12	0.2518	1.7467	1.5025	2.6245	0.0725	0.0274	0.0137						
12.5	0.2518	1.8195	1.5480	2.8166	0.0598	0.0233	0.0117						
13	0.2518	1.8923	1.5929	3.0143	0.0491	0.0197	0.0098						
13.5	0.2518	1.9651	1.6374	3.2177	0.0400	0.0165	0.0083						
14	0.2518	2.0378	1.6815	3.4266	0.0325	0.0138	0.0069						
14.5	0.2518	2.1106	1.7251	3.6411	0.0262	0.0114	0.0057						
15	0.2518	2.1834	1.7683	3.8610	0.0210	0.0094	0.0047					**0.9786**	
15.5	0.2518	2.2562	1.8112	4.0864	0.0168	0.0077	0.0038						

16	0.2518	2.3290	1.8537	4.3171	0.0133	0.0062	0.0031						
16.5	0.2518	2.4017	1.8958	4.5532	0.0105	0.0050	0.0025						
17	0.2518	2.4745	1.9375	4.7945	0.0083	0.0040	0.0020						
17.5	0.2518	2.5473	1.9790	5.0410	0.0065	0.0032	0.0016						
18	0.2518	2.6201	2.0201	5.2928	0.0050	0.0026	0.0013						
18.5	0.2518	2.6929	2.0609	5.5497	0.0039	0.0020	0.0010						
19	0.2518	2.7656	2.1014	5.8118	0.0030	0.0016	0.0008						
19.5	0.2518	2.8384	2.1416	6.0789	0.0023	0.0012	0.0006						
20	0.2518	2.9112	2.1816	6.3511	0.0017	0.0010	0.0005						**0.9959**
20.5	0.2518	2.9840	2.2213	6.6283	0.0013	0.0007	0.0004						
21	0.2518	3.0568	2.2607	6.9104	0.0010	0.0006	0.0003						
21.5	0.2518	3.1295	2.2999	7.1975	0.0007	0.0004	0.0002						
22	0.2518	3.2023	2.3388	7.4896	0.0006	0.0003	0.0002						
22.5	0.2518	3.2751	2.3775	7.7865	0.0004	0.0002	0.0001						
23	0.2518	3.3479	2.4159	8.0882	0.0003	0.0002	0.0001						
23.5	0.2518	3.4207	2.4542	8.3948	0.0002	0.0001	0.0001						
24	0.2518	3.4934	2.4922	8.7062	0.0002	0.0001	0.0001						
24.5	0.2518	3.5662	2.5300	9.0224	0.0001	0.0001	0.0000						
25	0.2518	3.6390	2.5675	9.3433	0.0001	0.0001	0.0000						

Probability of wind speed (in the 2.19 Mars year)

> 3.5 m/s	> 5m/s	> 7m/s	> 10 m/s	> 15 m/s	> 20 m/s
0.7040	**0.5335**	**0.3334**	**0.1354**	**0.0187**	**0.0014**

Figure S1. Photos of 0.25h, 1h, 3h, 7h ESD products from melanterite, $FeSO_4 \cdot 7H_2O$.

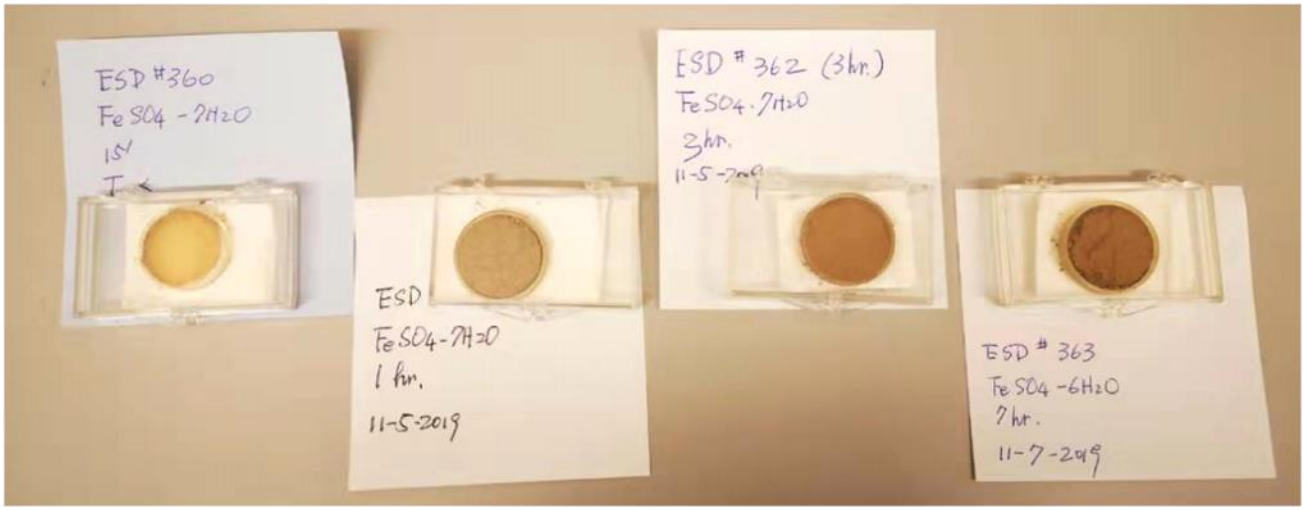

Figure S2. Photos of Na-jarosite after 35h and 64h ESD.

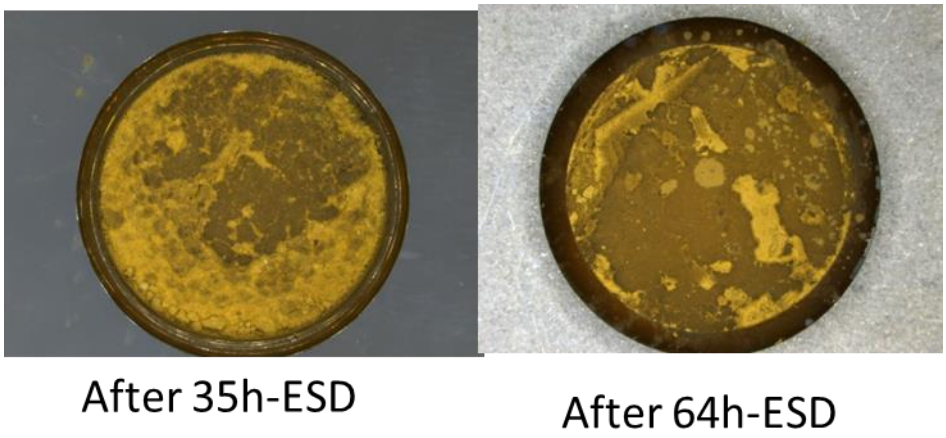

Figure S3. Raman spectra of 64h ESD product from Na-jarosite. Raman sampled spots are from dark area on *as is* surface.

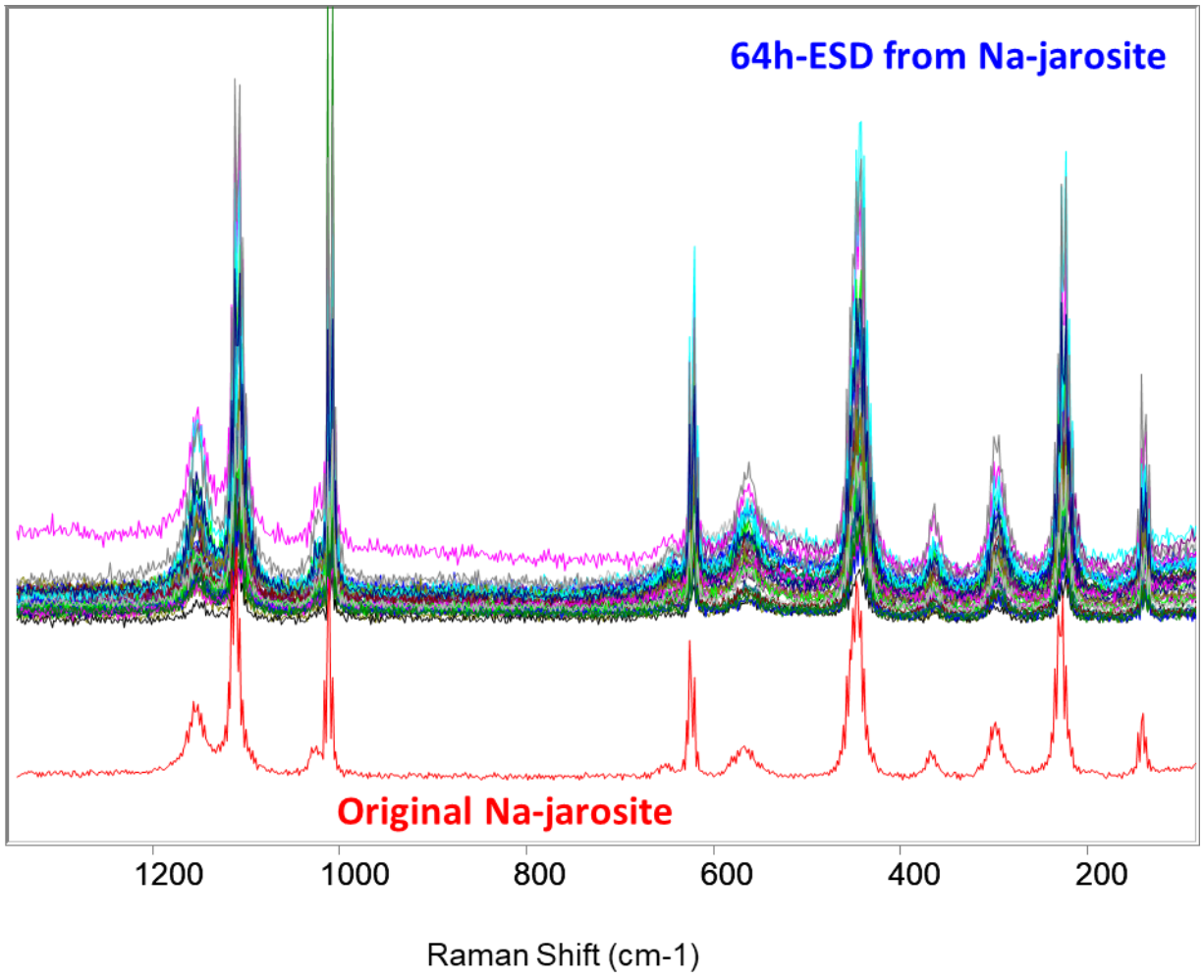

Figure S4. Mössbauer spectrum and curve fitting results of post 64h ESD jarosite.

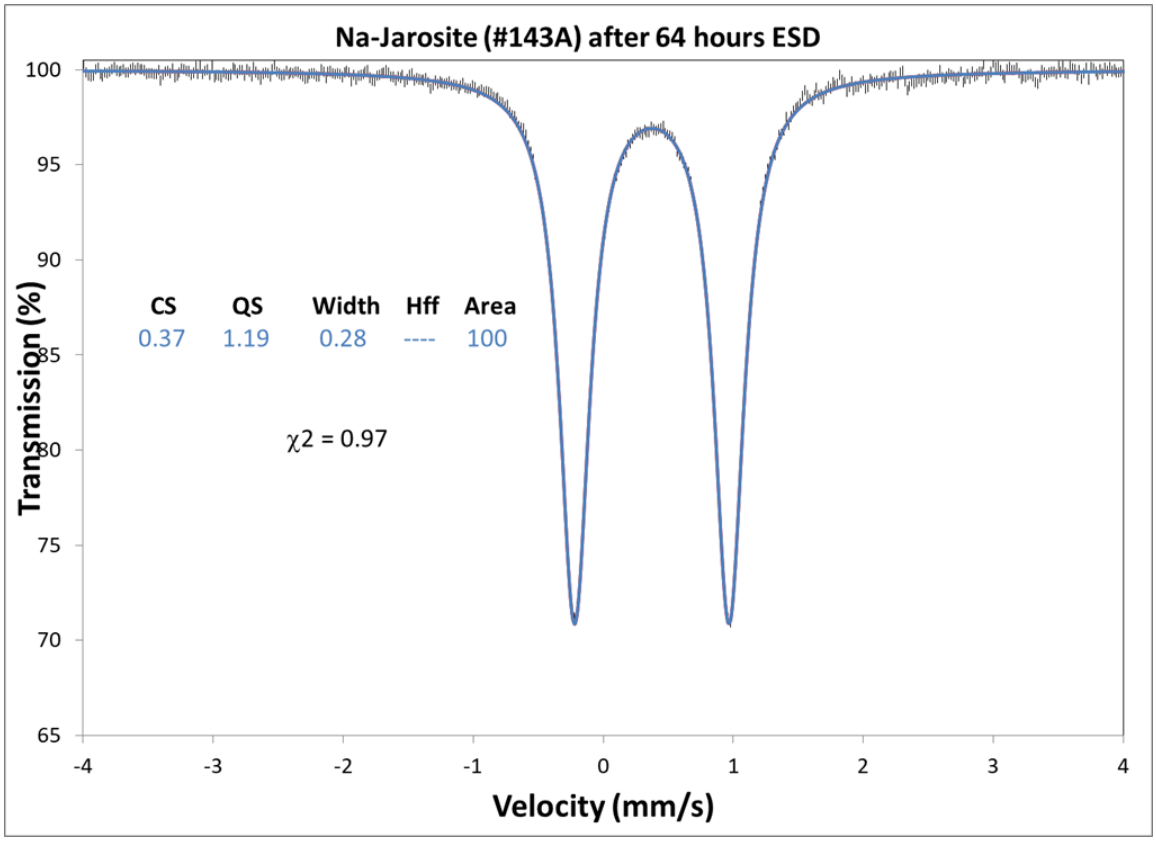

Figure S5. Raman spectra of 7h ESD product from akaganeite.

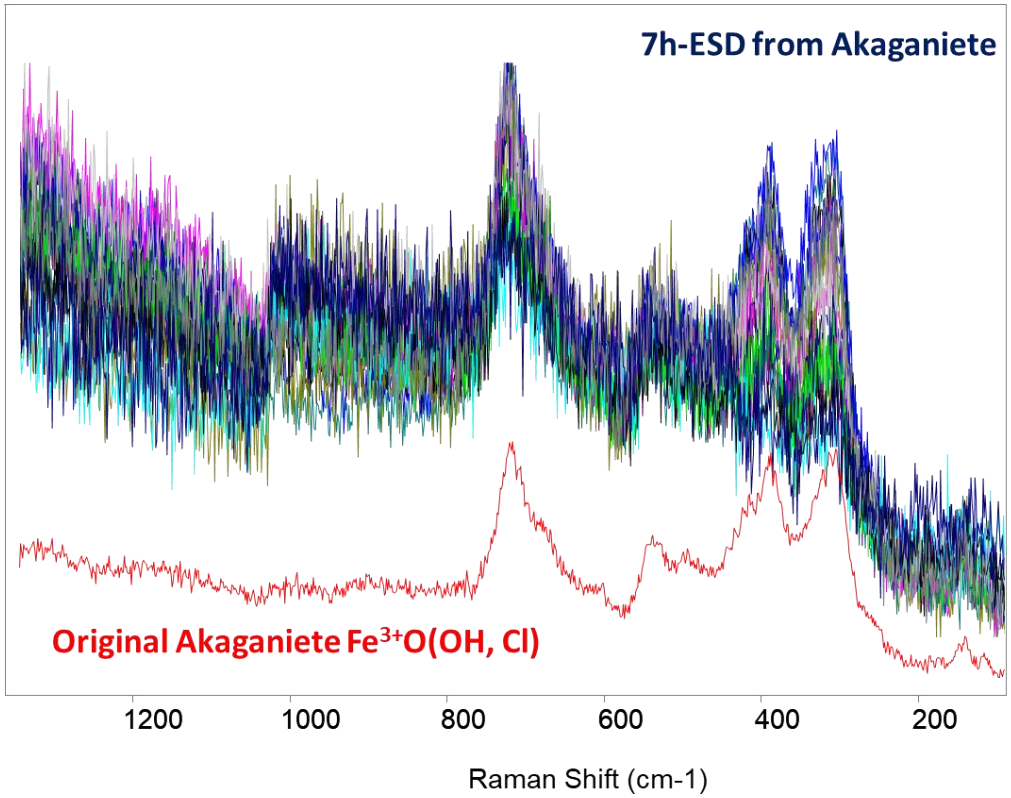

Figure S6. Raman spectra on *as is* surface of 14h ESD product from pyrite. They have the peak ranges of 378.5 – 368.8 (Δ =9.7) cm^{-1} and 342,0 – 337.0 (Δ=5.0) cm^{-1}; while the original natural pyrite sample (from Huanzala, Peru) has much narrow peak ranges of 379.8 – 374.6 (Δ=5.2) cm^{-1} and 344.4 – 340.6 (Δ =3.7) cm^{-1}. In addition, doublet occurs frequently in ESD products that does not exist in the spectra of original pyrite.

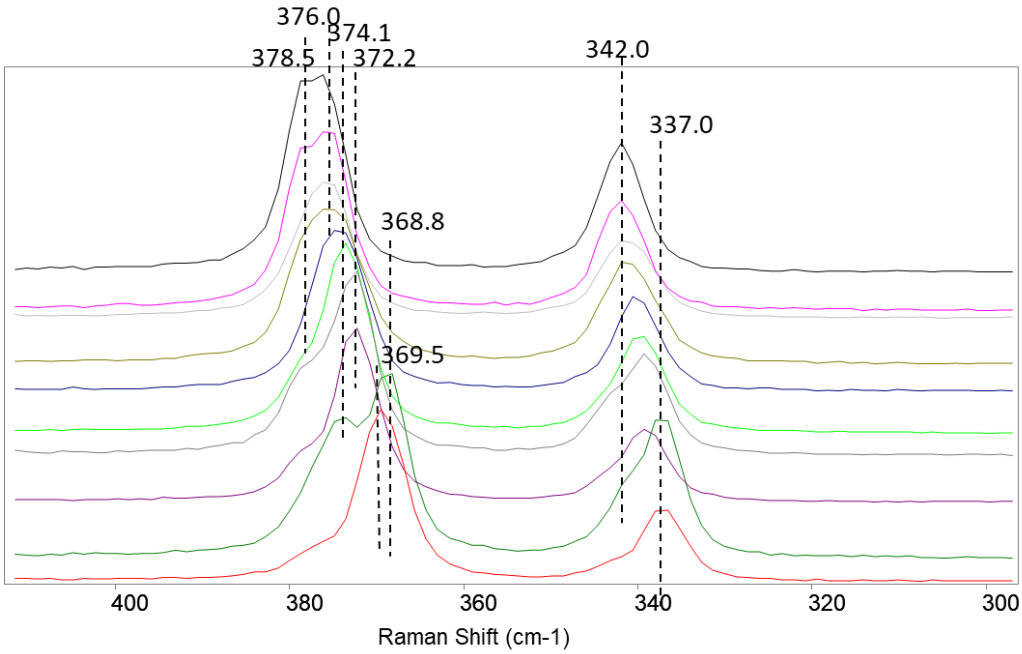

Figure S7. Three types of electrostatic discharge (Gallo 1975).

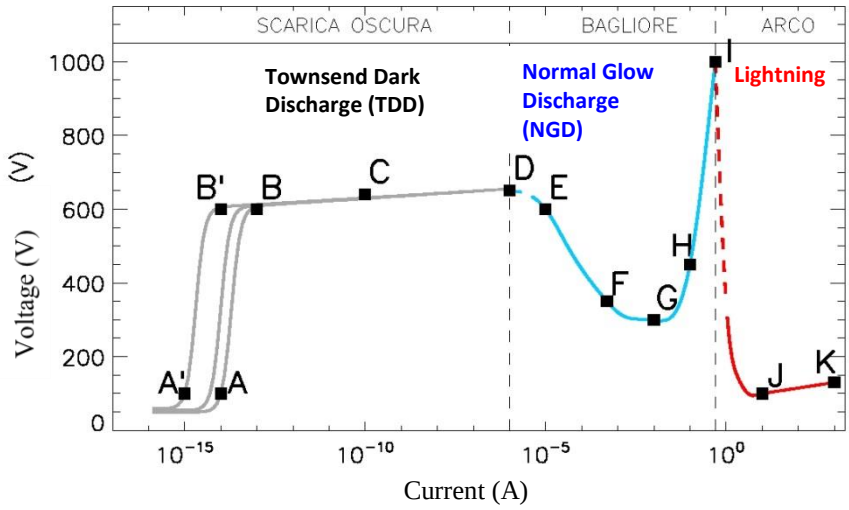

Figure S8 (from Figure 4 of Wu et al., 2018). Plasma emission spectra generated by ESD in PEACh within three different atmospheric environments at room temperature (a) in dry CO_2 (3.0 mbar); (b) in CO_2+H_2O (6.2 mbar, 7.2 %RH); (c) in Mars Simulate Gas Mixture (MSGM, CO_2 95%, N_2 2%, Ar 2%, O_2 1%, 3.0 mbar).